Article

# A Versatile Amino Acid Analogue of the Solvatochromic Fluorophore 4-*N*,*N*-Dimethylamino-1,8-naphthalimide: A Powerful Tool for the Study of Dynamic Protein Interactions

Galen Loving, and Barbara Imperiali

*J. Am. Chem. Soc.*, **2008**, 130 (41), 13630-13638 • DOI: 10.1021/ja804754y • Publication Date (Web): 23 September 2008



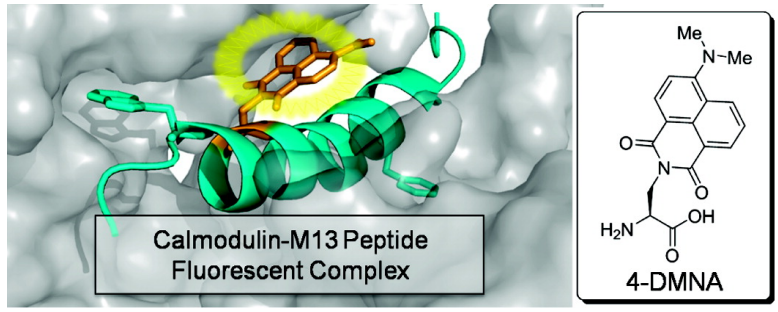


## More About This Article

Additional resources and features associated with this article are available within the HTML version:

- Supporting Information
- Access to high resolution figures
- Links to articles and content related to this article
- Copyright permission to reproduce figures and/or text from this article

View the Full Text HTML

J|A|C|S
ARTICLES

Published on Web 09/23/2008

# A Versatile Amino Acid Analogue of the Solvatochromic Fluorophore 4-*N,N*-Dimethylamino-1,8-naphthalimide: A Powerful Tool for the Study of Dynamic Protein Interactions

Galen Loving and Barbara Imperiali*

*Departments of Chemistry and Biology, Massachusetts Institute of Technology, 77 Mass Avenue, Cambridge, Massachusetts 02139*

Received June 21, 2008; E-mail: imper@mit.edu

***Abstract:*** We have developed a new unnatural amino acid based on the solvatochromic fluorophore 4-*N,N*-dimethylamino-1,8-naphthalimide (4-DMN) for application in the study of protein−protein interactions. The fluorescence quantum yield of this chromophore is highly sensitive to changes in the local solvent environment, demonstrating "switch-like" emission properties characteristic of the dimethylaminophthalimide family of fluorophores. In particular, this new species possesses a number of significant advantages over related fluorophores, including greater chemical stability under a wide range of conditions, a longer wavelength of excitation (408 nm), and improved synthetic accessibility. This amino acid has been prepared as an Fmoc-protected building block and may readily be incorporated into peptides via standard solid-phase peptide synthesis. A series of comparative studies are presented to demonstrate the advantageous properties of the 4-DMN amino acid relative to those of the previously reported 4-*N,N*-dimethylaminophthalimidoalanine and 6-*N,N*-dimethylamino-2,3-naphthalimidoalanine amino acids. Other commercially available solvatochromic fluorophores are also include in these studies. The potential of this new probe as a tool for the study of protein−protein interactions is demonstrated by introducing it into a peptide that is recognized by calcium-activated calmodulin. The binding interaction between these two components yields an increase in fluorescence emission greater than 900-fold.

## Introduction

Dynamic protein−protein interactions within the cell play a critical and pervasive role in nature. Many signal transduction pathways are mediated through the binding and dissociation of key proteins in a tightly regulated fashion.[1] The dynamics of these interactions are also vital to the controlled assembly and disassembly of many functional ensembles, such as the actin filament component of the cytoskeleton[2] or the focal adhesions involved in mammalian cell migration.[3] As such, concentrated efforts to better understand these interactions have led to the development of a wide range of techniques that are now commonplace in the field of protein biochemistry. These techniques span a broad spectrum from purely *in vitro* biophysical methods, such as isothermal titration calorimetry[4] and analytical ultracentrifugation,[5] to ones more amenable to *in cellulo* studies, like yeast two-hybrid assays[6] and photoaffinity labeling.[7] While each of the approaches is indispensible for the unique information that it provides, many of these methods are limited in the ability to yield spatial and temporal information regarding dynamic interactions and are often necessarily destructive to the cell. Consequently, a vast number of questions regarding the temporal and spatial significance of various protein−protein interactions within living cells remain unanswered and require a new generation of tools if further advances are to be made.

An ideal tool for addressing these questions should be one that can sensitively detect the transient nature of various protein−protein interactions in a reversible manner. By this measure, Förster resonance energy transfer (FRET) has become increasingly popular in the literature and stands as one of the preferred methods for *in cellulo* studies.[8] An alternative approach is the use of solvatochromic fluorophores, which feature emission properties that exhibit a significant dependence on changes in solvent polarity, solvent relaxation rates, orientation to electric fields, and rigidity of the local environment.[9] The effects of these environmental factors on the photophysical attributes of the fluorophore typically manifest as a shift in the wavelength of maximum emission or a change in magnitude of the observed fluorescence lifetime or quantum yield. In many instances all three properties, which constitute the dynamic range of the fluorophore, are affected simultaneously.

Over the past few years our group has developed and investigated the application of novel amino acids that possess

(1) Pawson, T.; Nash, P. *Science* **2003**, *300*, 445–452.
(2) Vicente-Manzanares, M.; Webb, D. J.; Horwitz, A. R. *J. Cell Sci.* **2005**, *118*, 4917–4919.
(3) Zamir, E.; Geiger, B. *J. Cell Sci.* **2001**, *114*, 3583–3590.
(4) Velazquez-Campoy, A.; Ohtaka, H.; Nezami, A.; Muzammil, S.; Freire, E. *Curr. Protoc. Cell. Biol.* **2004**, *17*, 17–18.
(5) Lebowitz, J.; Lewis, M. S.; Schuck, P. *Protein Sci.* **2002**, *11*, 2067–2079.
(6) Young, K. H. *Biol. Reprod.* **1998**, *58*, 302–311.
(7) Dormán, G. *Bioorganic Chemistry of Biological Signal Transduction*; Springer-Verlag Berlin: Heidelberg, 2001; pp169−225.
(8) Jares-Erijman, E. A.; Jovin, T. M. *Nat. Biotechnol.* **2003**, *21*, 1387–1395.
(9) Lakowicz, J. R. *Principles of Fluorescence Spectroscopy*, 3rd ed.; Springer: New York, 2006.


**10.1021/ja804754y CCC: $40.75** 

***Chart 1.*** Dimethylaminophthalimidoalanine Series of Solvatochromic Amino Acids

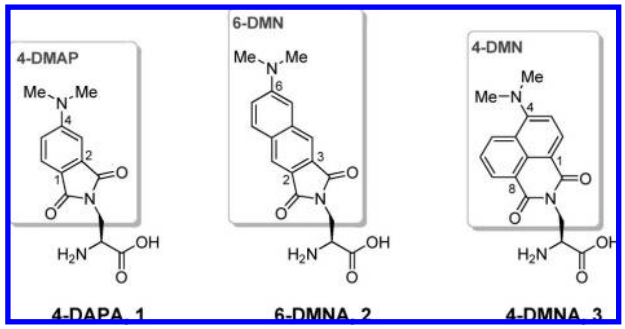


solvatochromic fluorophores as the side-chain group.[10−13] Amino acid derivatives of 4-*N,N*-dimethylaminophthalimide (4-DMAP) and 6-*N,N*-dimethylamino-2,3-naphthalimide (6-DMN) are of particular interest (Chart 1) due to the exceptionally low fluorescence quantum yields that they exhibit in polar protic solvents such as water compared to those in nonpolar solvents. This offers the advantage of a greater signal-to-noise ratio over those obtained with other commercially available solvatochromic fluorophores. With sizes comparable to tryptophan, the fluorescent amino acid analogues, 4-*N,N*-dimethylaminophthalimidoalanine (4-DAPA, **1**) and 6-*N,N*-dimethylamino-2,3-naphthalimidoalanine (6-DMNA, **2**), can be incorporated into the primary sequence of a peptide or protein without introducing a significant perturbation to the overall surface topology of the native structure. The 4-DAPA and 6-DMNA amino acids have been incorporated into peptide motifs that are recognized by 14-3-3 proteins,[11] SH2 domains,[12] PDZ domains, opioid receptors,[14] and the class II MHC proteins[13] and have proven very effective as probes for monitoring binding. However, due to the intrinsic strain of the five-membered phthalimide ring systems of 4-DMAP and 6-DMN, these fluorophores are susceptible to nucleophilic attack, leading to the formation of ring-opened byproducts.

Recently, we have developed a new solvatochromic amino acid, 4-*N,N*-dimethylamino-1,8-naphthalimidoalanine (4-DMNA, **3**), to complement 4-DAPA and 6-DMNA. This amino acid offers several distinct advantages over the previous two while retaining many of the same excellent solvatochromic properties that are characteristic of the dimethylaminophthalimide series. The six-membered imide ring of 4-*N,N*-dimethylamino-1,8-naphthalimide (4-DMN, Chart 1) eliminates angle strain on the $sp^2$-hybridized nuclei, resulting in much greater chemical stability.

The earliest reports of the fluorescent properties of 4-DMN can be traced to studies involving derivatives of the parent 4-amino-1,8-naphthalimide group, which were beginning to draw interest for their brilliant yellow and orange colors.[15] Since that time, the fluorophore has been utilized in a wide range of technologies,[16−18] and its photophysical properties have been studied extensively.[19−24] However, biological applications of 4-DMN are comparatively scarce.[25−27]

***Scheme 1.*** Synthesis of Fmoc-Protected 4-DMNA (**4**)[a]

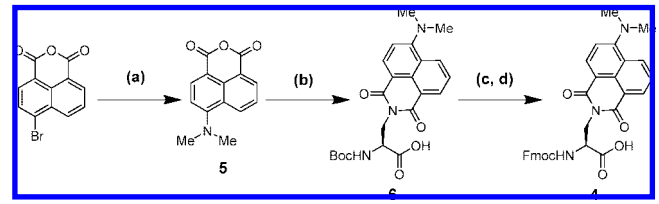


[a] Reagents and conditions: (a) 3-dimethylaminopropionitrile, 3-methyl-1-butanol, Δ, $N_2$ (1 atm), 12 h, quantitative yield;[19] (b) $NaHCO_3$, 3-amino-2-(Boc-amino)-propionic acid, dioxane/water (5:1), Δ, $N_2$ (1 atm), 30 min, 55% yield; (c) TFA/DCM (1:1), 23 °C, 1.5 h; (d) Fmoc-OSu, $NaHCO_3$, dioxane/$H_2O$ (5:1), 23 °C, 2 h, 83% overall yield for steps c and d.

The experiments described herein demonstrate the potential of this solvatochromic fluorophore as a tool for detecting biomolecular interactions. The improved stability, the ease of synthesis, and the longer wavelength of excitation of **3** over those of the amino acids **1** and **2** will greatly expand the range of potential applications. A comparative study is provided that evaluates the properties of 4-DMN relative to those of 6-DMN and 4-DMAP as well as other frequently used solvatochromic fluorophores that are commercially available: BADAN, dansyl, and NBD.[28]

## Results and Discussion

**Synthesis of the *N*-α-Fmoc-(4-*N,N*-Dimethylamino-1,8-naphthalimido)alanine Building Block (4).** Preparation of the Fmoc-protected 4-DAPA and 6-DMNA amino acids both required multistep syntheses. By contrast, the synthetic route that gives **4** is relatively short, requiring only four steps (Scheme 1). This approach allows facile access to gram quantities of material with high purity. The procedure begins with the preparation of the anhydride precursor of 4-DMN, **5**, performed according to the method described by Kollár et al.[19] Once obtained, the anhydride is then condensed with 3-amino-2-(Boc-amino)propionic acid under an atmosphere of $N_2$ to prevent oxidation of the aniline

(10) Nitz, M.; Mezo, A. R.; Ali, M. H.; Imperiali, B. *Chem. Commun. (Cambridge, U.K.)* **2002**, 1912–1913.
(11) Vazquez, M. E.; Rothman, D. M.; Imperiali, B. *Org. Biomol. Chem.* **2004**, *2*, 1965–1966.
(12) Vazquez, M. E.; Blanco, J. B.; Imperiali, B. *J. Am. Chem. Soc.* **2005**, *127*, 1300–1306.
(13) Venkatraman, P.; Nguyen, T. T.; Sainlos, M.; Bilsel, O.; Chitta, S.; Imperiali, B.; Stern, L. J. *Nat. Chem. Biol.* **2007**, *3*, 222–228.
(14) Vazquez, M. E.; Blanco, J. B.; Salvadori, S.; Trapella, C.; Argazzi, R.; Bryant, S. D.; Jinsmaa, Y.; Lazarus, L. H.; Negri, L.; Giannini, E.; Lattanzi, R.; Colucci, M.; Balboni, G. *J. Med. Chem.* **2006**, *49*, 3653–3658.
(15) Alexiou, M. S.; Tychopoulos, V.; Ghorbanian, S.; Tyman, J. H. P.; Brown, R. G.; Brittain, P. I. *J. Chem. Soc., Perkin Trans. 2* **1990**, 837–842.
(16) Grabchev, I.; Meallier, P.; Konstantinova, T.; Popova, M. *Dyes Pigments* **1995**, *28*, 41–46.
(17) Tomasz, M.; Krzysztof, F.; Hanka, M.; Ewa, M.; Eryk, W.; Danuta, B.; Jozef, Z. *Proc. SPIE: Int. Soc. Opt. Eng.* **1995**, *2372*, 317–322.
(18) Jun, L.; Changchun, M.; Quanguo, Z.; Yanxiang, C.; Lixiang, W.; Dongge, M.; Xiabin, J.; Fosong, W. *Appl. Phys. Lett.* **2006**, *88*, 083505.
(19) Kollár, J.; Hrdlovic, P.; Chmela, S.; Sarakha, M.; Guyot, G. *J. Photochem. Photobiol., A* **2005**, *170*, 151–159.
(20) Saha, S.; Samanta, A. *J. Phys. Chem. A* **2002**, *106*, 4763–4771.
(21) Grabchev, I.; Guittonneau, S.; Konstantinova, T.; Meallier, P. *Bull. Soc. Chim. Fr.* **1994**, *131*, 828–830.
(22) Zhang, W.; Wang, Y. L.; Xu, Y. F.; Qian, X. H. *Monatsh. Chem.* **2003**, *134*, 393–402.
(23) Banthia, S.; Samanta, A. *Chem. Lett.* **2005**, *34*, 722–723.
(24) Grabtchev, I.; Philipova, T.; Meallier, P.; Guittonneau, S. *Dyes Pigments* **1996**, *31*, 31–34.
(25) Berque-Bestel, I.; Soulier, J. L.; Giner, M.; Rivail, L.; Langlois, M.; Sicsic, S. *J. Med. Chem.* **2003**, *46*, 2606–2620.
(26) Singh, S.; Singh, R. *J. Fluoresc.* **2007**, *17*, 139–148.
(27) Gryzunov Iu, A.; Miller Iu, I.; Dobretsov, G. E.; Pestova, A. B. *Klin. Lab. Diagn.* **1994**, 27–31.
(28) Reactive derivatives of these three fluorophores are availiable through a number of companies such as Molecular Probes and AnaSpec, Inc.

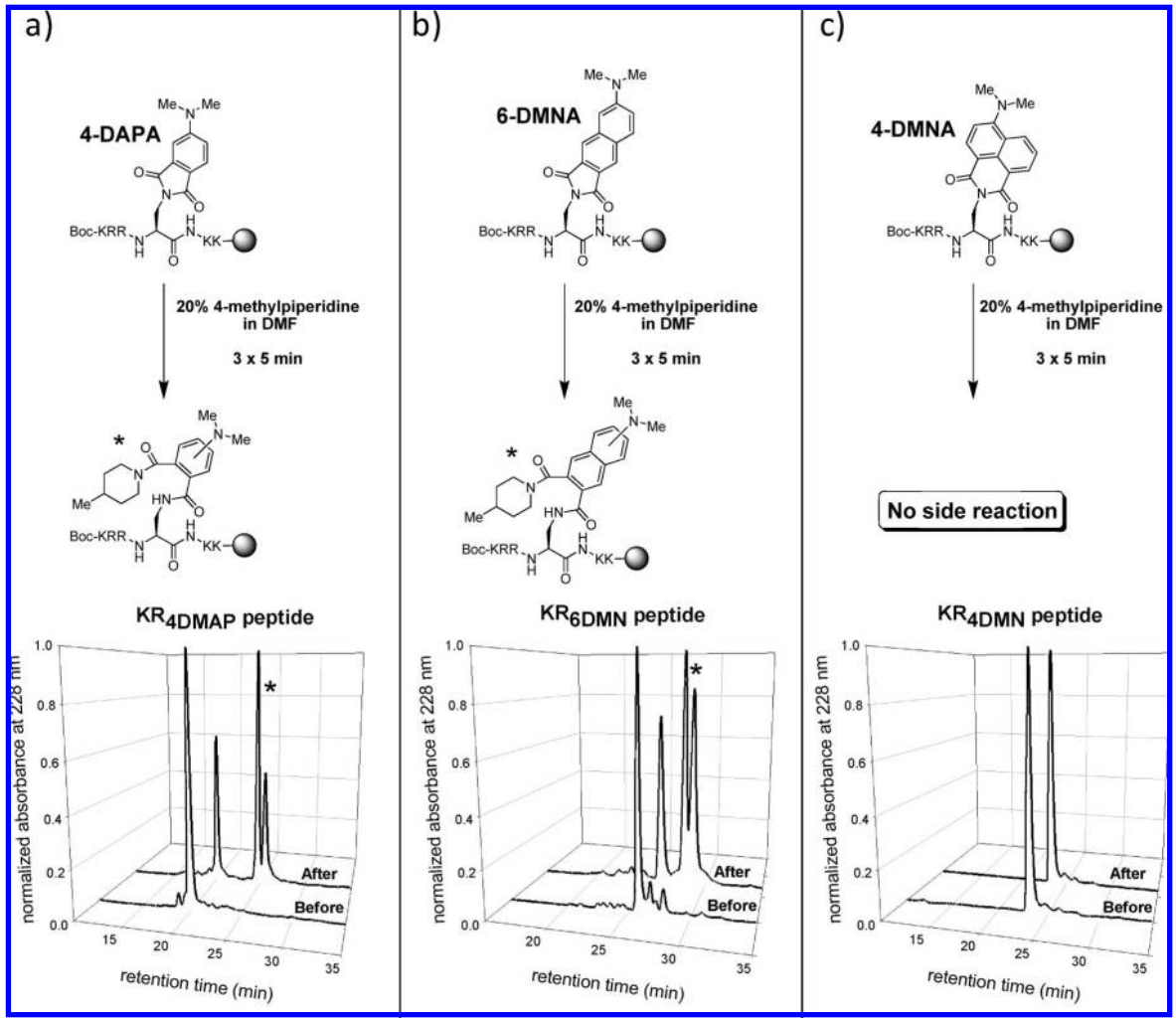


***Figure 1.*** (a,b) Illustration of the susceptibility of the amino acids 4-DAPA and 6-DMNA to nucleophilic attack by bases such as 4-methylpiperidine, leading to ring-opened byproducts. The HPLC traces (bottom) depict the model KR peptides cleaved before and after exposure to the base. The addition of 4-methylpiperidine to the imide rings of 4-DMAP and 6-DMN gives a mixture of two regioisomers (*) as shown in the HPCL traces after treatment. (c) The amino acid, 4-DMNA, exhibits no sign of degradation under these same conditions. The identities of the peaks were determined by a combination of MALDI and ESI mass spectrometry.

nitrogen while refluxing. The Boc group of **6** is then removed under acidic conditions before treatment with *N*-(9-fluorenylmethoxycarbonyloxy)succinimide (Fmoc-OSu) under basic conditions to give the final product **4** in good yield (see Supporting Information for details).

**Compatibility of the Fmoc-4DMNA Amino Acid (4) with Standard Solid-Phase Peptide Synthesis.** A significant drawback to the use of 4-DAPA and 6-DMNA in solid-phase peptide synthesis (SPPS) is their reactivity toward nucleophilic bases such as piperidine, which are commonly used for Fmoc group deprotection. While the formation of ring-opened piperidine adducts of these two amino acids can be circumvented by substituting piperidine with 1,8-diazabicyclo[5.4.0]undec-7-ene (DBU),[29] caution must be exercised with sequences containing certain Asp-Xaa motifs due to the potential for aspartimide formation.[30] By contrast, the Fmoc amino acid of 4-DMNA, **4**, has been used for the preparation of a number of fluorescent peptides and shows no susceptibility to piperidine. The following experiment illustrates the enhanced stability of 4-DMNA by treating a series of model peptides ($KR_{4DMAP}$, $KR_{6DMN}$, and $KR_{4DMN}$) with 4-methylpiperidine[31] while still bound to the solid support (Figure 1). The conditions used simulate a standard Fmoc-deprotection cycle. Samples of the treated and untreated peptides were then cleaved from the resin under acidic conditions, and the crude mixtures were analyzed by HPLC and mass spectrometry (see Supporting Information for details).

The HPLC traces in Figure 1a,b clearly exhibit the presence of two new peaks that elute later than that of the desired product after treatment with 4-methylpiperidine. These new peaks correspond to the masses of the ring-opened adducts that occur as a mixture of regioisomers. By contrast, the $KR_{4DMN}$ peptide yielded virtually identical HPLC traces before and after treatment with 4-methylpiperidine and showed no signs of degradation (Figure 1c). The robustness of 4-DMNA allows for multiple Fmoc-deprotection cycles to be performed subsequent to its incorporation into a peptide, obviating the need for the use of bases like DBU.

**Stability of 4-DMNA (3) to Hydrolysis.** Very often proteins are limited to a narrow range of conditions in which they are

(29) Sainlos, M.; Imperiali, B. *Nat. Protoc.* **2007**, *2*, 3210–3218.
(30) Wade, J. D.; Mathieu, M. N.; Macris, M.; Tregear, G. W. *Lett. Pept. Sci.* **2000**, *7*, 107–112.
(31) Hachmann, J.; Lebl, M. *J. Comb. Chem.* **2006**, *8*, 149.

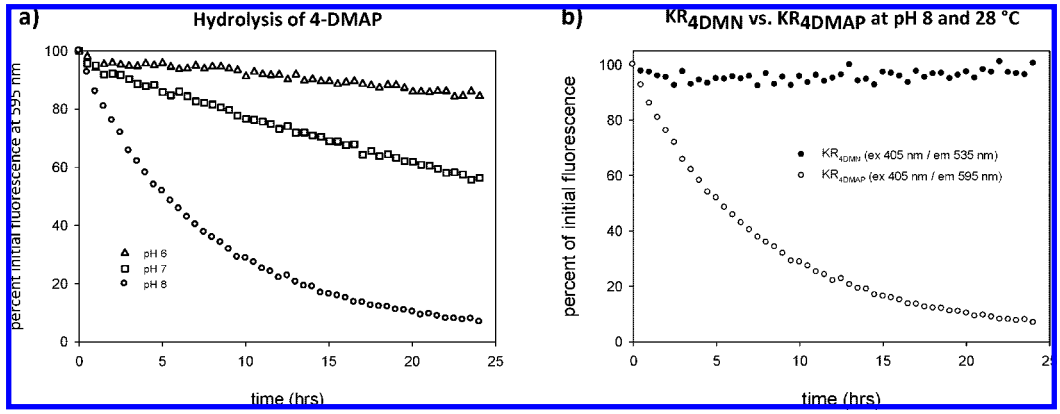


***Figure 2.*** (a) Loss of fluorescence due to imide ring hydrolysis of 4-DMAP in the $KR_{4DMAP}$ peptide (40 $\mu$M) over 24 h in PBS buffer at 28 °C. The data reveal the rate enhancement observed at higher pH levels. (b) Side-by-side comparison of 4-DMN versus 4-DMAP, showing that no significant change in fluorescence was observed for 4-DMN under the harshest conditions anticipated for its use. No hydrolysis byproduct was detected by ESI MS for the treated $KR_{4DMN}$ peptide.

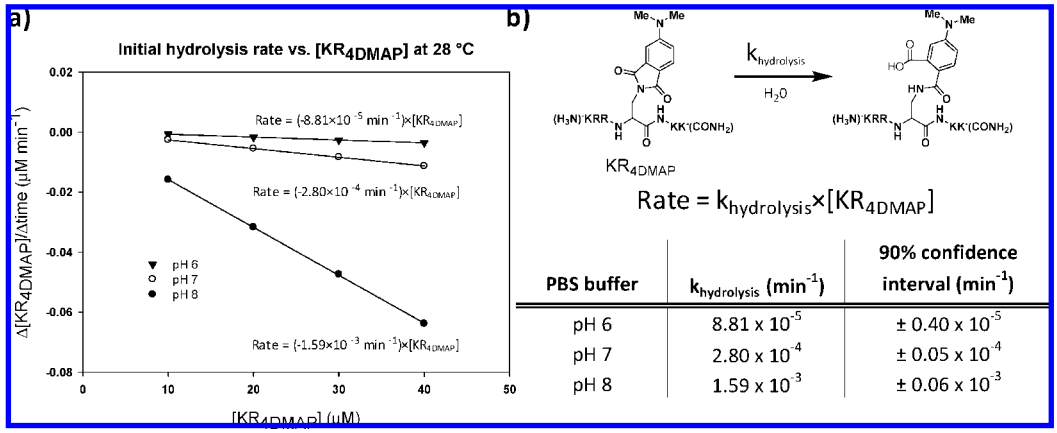


***Figure 3.*** (a) Pseudo-first-order dependence of the hydrolysis of 4-DMAP based on the initial rates measured at four concentrations of the $KR_{4DMAP}$ peptide. The reaction was examined at three different pH levels (pH 6, 7, and 8). Regression lines were set to intercept the *y*-axis at zero. (b) Calculated rate constants for the hydrolysis of the $KR_{4DMAP}$ peptide with the reaction scheme and rate law (omitting the contribution of $[H_2O]$) depicted above.

stable or functional (pH, temperature, detergents, etc.). Because these conditions are sometimes extremely restrictive, it is important to have fluorescent tools devoid of additional environmental constraints. A principal vulnerability of the 4-DMAP and 6-DMN fluorophores is the tendency to hydrolyze over time at high pH. While hydrolysis of the imide ring of 4-DMAP leads to a nonfluorescent byproduct, the hydrolysis of 6-DMN results in a fluorescent species with an emission maximum observed at 470−480 nm. This produces a gradual increase in background fluorescence, eventually reducing the signal-to-noise ratio.

A comparison of 4-DMAP with 4-DMN was performed to demonstrate the enhanced stability of 4-DMN toward hydrolysis. The $KR_{4DMAP}$ peptide was screened at various concentrations in PBS buffer at three different pH levels (pH 6, 7, and 8). Since 4-DMAP undergoes a loss of fluorescence upon hydrolysis, the percent conversion of the fluorophore can be defined as the percent loss of fluorescence from time zero. These same conditions were also applied to the $KR_{4DMN}$ peptide. The reactions were monitored in a 96-well plate over the course of 24 h (see Supporting Information for details).

Here, a clear trend emerges from the data of the $KR_{4DMAP}$ peptide. The rate of hydrolysis is relatively modest at low pH but increases considerably as the pH is raised (Figures 2 and 3). By measuring the initial rates at four different concentrations of the peptide, a pseudo first-order rate constant was computed for the reaction at each pH level (Figure 3). The results of this experiment were comparable to those measured for the $KR_{6DMN}$ peptide, indicating that the imide ring size was the dominant driving force for the observed reactivity and that the proximity of the dimethylamino group bears little impact on the rate of reaction (see Supporting Information for details). By comparison, the $KR_{4DMN}$ peptide showed no signs of degradation under any of the applied conditions. This is especially apparent in Figure 2b, where the fluorescence emission of the $KR_{4DMN}$ peptide was unchanged after 24 h while the fluorescent signal from the $KR_{4DMAP}$ peptide was almost completely abolished.

**Comparison of the Solvatochromic Properties of the *N,N*-Dimethylaminophthalimide Series with BADAN, Dansyl, and NBD.** Since their discovery, reactive derivatives of solvatochromic fluorophores like dansyl chloride (5-(dimethylamino)-naphthalene-1-sulfonyl chloride),[32,33] BADAN (6-bromoacetyl-2-dimethylaminonaphthalene),[10,34,35] and NBD fluoride (4-fluoro-7-nitrobenzofurazan)[36−38] have been used extensively in

(32) Zuhlke, R. D.; Pitt, G. S.; Deisseroth, K.; Tsien, R. W.; Reuter, H. *Nature* **1999**, *399*, 159–162.
(33) Torok, K.; Cowley, D. J.; Brandmeier, B. D.; Howell, S.; Aitken, A.; Trentham, D. R. *Biochemistry* **1998**, *37*, 6188–6198.
(34) Tsalkova, T. N.; Davydova, N. Y.; Halpert, J. R.; Davydov, D. R. *Biochemistry* **2007**, *46*, 106–119.
(35) Zhang, J.; Wallar, B. J.; Popescu, C. V.; Renner, D. B.; Thomas, D. D.; Lipscomb, J. D. *Biochemistry* **2006**, *45*, 2913–2926.

***Chart 2.*** KR Peptide Series of Solvatochromic Fluorophores

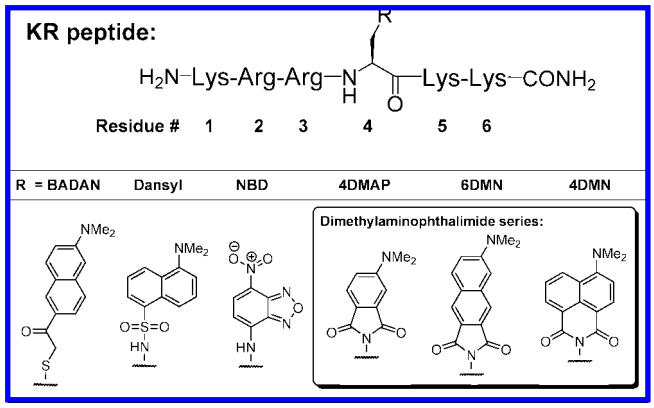


the areas of cell biology and protein biochemistry. All three exhibit hypsochromic shifts (blue shifts) in the emission spectra upon changing from a polar to nonpolar environment. Additionally, these display greater fluorescence quantum yields in hydrophobic solvents than in aqueous buffers. The same trends also apply to the dimethylaminophthalimide series, although these probes have the notable advantage of possessing much larger differences in fluorescence quantum yields in response to the solvent environment.

To evaluate the properties of 4-DMNA, we incorporated it into a test peptide via SPPS. We also prepared the same peptide with the amino acids of 4-DMAP, 6-DMN, BADAN, dansyl, and NBD. Each member of the series contained one of the six fluorophores located at the fourth position within a six-residue sequence rich in lysine and arginine residues (hence dubbed the KR peptide series in reference to the one-letter amino acid code, Chart 2). The peptides were studied in different solvent systems (dioxane and water) to encompass a broad range of the solvent polarity spectrum. The KR peptide motif was selected specifically to ensure complete solubility of the fluorophores in both solvent systems for accurate fluorescence measurements. While the highly charged peptides are naturally soluble in aqueous buffers such as TBS (pH 7.4), the peptides can easily be dissolved in dioxane in the presence of 18-crown-6, which forms very strong complexes with protonated primary amines such as those of the lysine residues and N-terminus (see Supporting Information for details).

The most striking trend to emerge from this study was the substantial difference in fluorescence intensities exhibited by the dimethylaminophthalimide series between the two solvent systems. In each case, the ratio of the fluorescence intensity was greater than 1000-fold (Table 1). This was significantly greater than that observed for dansyl and NBD. The magnitude of this ratio is attributed primarily to the extremely low fluorescence quantum yields of the dimethylaminophthalimides in polar protic solvents, creating the appearance of virtually no fluorescence in TBS buffer as plotted in the graphs of Figure 4. BADAN, a derivative of PRODAN[39] that has long been considered state-of-the-art for applications in biological studies, also displayed a formidable fluorescent response between water

***Table 1.*** Photophysical Properties of the Fluorescent KR Peptide Series

| peptide | $\lambda_{abs}$ (nm) | $\epsilon$ ($M^{-1}$ $cm^{-1}$) | $\lambda_{exc}$ (nm) | $\lambda_{em}$ (nm), TBS | $\lambda_{em}$ (nm), dioxane | $I_{dioxane}/I_{TBS}$ at $\lambda_{em}$ in dioxane[a] |
|---|---|---|---|---|---|---|
| $KR_{4DMAP}$ | 421 | $6.5 \times 10^3$ | 390 | 580 | 497 | $4.5 \times 10^3 \pm 1.4 \times 10^3$ |
| $KR_{4DMN}$ | 440 | $8.8 \times 10^3$ | 408 | 554 | 512 | $1.2 \times 10^3 \pm 0.2 \times 10^3$ |
| $KR_{6DMN}$ | 390 | $8.0 \times 10^3$ | 378 | 625 | 520 | $1.4 \times 10^3 \pm 0.2 \times 10^3$ |
| $KR_{BADAN}$ | 391 | $2.0 \times 10^4$ | 365 | 550 | 457 | $7.0 \times 10^2 \pm 0.2 \times 10^2$ |
| $KR_{dansyl}$ | 337 | $5.3 \times 10^3$ | 345 | 564 | 499 | $66 \pm 1$ |
| $KR_{NBD}$ | 465 | $2.2 \times 10^4$ | 455 | 543 | 523 | $7.0 \pm 0.3$ |

[a] This ratio was calculated by integrating the fluorescence intensity in both solvent systems over a 5 nm window centered on the wavelength of maximum emission in dioxane. The area of the measured region in dioxane was then divided by that measured in TBS buffer. The listed errors represent the 90% confidence interval from three trials.

and dioxane, despite its large quantum yield of fluorescence in water ($\Phi_{water} = 0.18$).[40] However, even with this excellent performance under these idealized conditions, such absolute changes are rarely achieved in actual biological applications. This experiment merely demonstrates the potential dynamic range of each fluorophore under optimal conditions. In protein studies, where the conditions are typically far from optimal, even the smallest degree of background fluorescence can strongly limit the magnitude of the observed fluorescence change.

**Preparation of M13 Peptide Mutants and Binding Studies with Calmodulin.** To examine the behavior of these fluorophores in a more biologically relevant context, another peptide series was prepared (Table 2). This series was derived from the previously reported M13 peptide,[41] which contains the calmodulin binding domain of skeletal muscle myosin light chain kinase (skMLCK). Calmodulin (CaM) binds the M13 peptide in a calcium-dependent manner with a reported $K_d$ on the order of $10^{-9}-10^{-10}$ M.[42] The structural details of this interaction have been extremely well characterized and shown to form many hydrophobic contacts as the protein literally wraps around the peptide binding partner (Figure 5).[42] Hence, the calcium-dependent CaM−M13 interaction has served as a model system for evaluating many new methods for detecting protein−protein interactions.[43−46]

Based on the structural information available for the $Ca^{2+}$-CaM-M13 complex, the phenylalanine residue located at position 8 of the wild-type M13 sequence was selected as the site for introducing the fluorescent probes. This residue is known to make a number of hydrophobic contacts with $Ca^{2+}$-CaM. Furthermore, reports of other peptide sequences that bind CaM through a mode similar to that of the M13 peptide have shown

(36) Ding, F. X.; Lee, B. K.; Hauser, M.; Davenport, L.; Becker, J. M.; Naider, F. *Biochemistry* **2001**, *40*, 1102–1108.
(37) Hagihara, M.; Fukuda, M.; Hasegawa, T.; Morii, T. *J. Am. Chem. Soc.* **2006**, *128*, 12932–12940.
(38) Wang, Q. Z.; Lawrence, D. S. *J. Am. Chem. Soc.* **2005**, *127*, 7684–7685.
(39) Weber, G.; Farris, F. J. *Biochemistry* **1979**, *18*, 3075–3078.
(40) Prendergast, F. G.; Meyer, M.; Carlson, G. L.; Iida, S.; Potter, J. D. *J. Biol. Chem.* **1983**, *258*, 7541–7544.
(41) Blumenthal, D. K.; Takio, K.; Edelman, A. M.; Charbonneau, H.; Titani, K.; Walsh, K. A.; Krebs, E. G. *Proc. Natl. Acad. Sci. U.S.A.* **1985**, *82*, 3187–3191.
(42) Ikura, M.; Clore, G. M.; Gronenborn, A. M.; Zhu, G.; Klee, C. B.; Bax, A. *Science* **1992**, *256*, 632–638.
(43) Kawahashi, Y.; Doi, N.; Takashima, H.; Tsuda, C.; Oishi, Y.; Oyama, R.; Yonezawa, M.; Miyamoto-Sato, E.; Yanagawa, H. *Proteomics* **2003**, *3*, 1236–1243.
(44) Ozawa, T.; Nogami, S.; Sato, M.; Ohya, Y.; Umezawa, Y. *Anal. Chem.* **2000**, *72*, 5151–5157.
(45) Ozawa, T.; Umezawa, Y. *Curr. Opin. Chem. Biol.* **2001**, *5*, 578–583.
(46) Kajihara, D.; Abe, R.; Iijima, I.; Komiyama, C.; Sisido, M.; Hohsaka, T. *Nat. Methods* **2006**, *3*, 923–929.
(47) Crivici, A.; Ikura, M. *Annu. Rev. Biophys. Biomol. Struct.* **1995**, *24*, 85–116.
(48) This structure rendered using PyMol v0.99 (DeLano Scientific LLC).

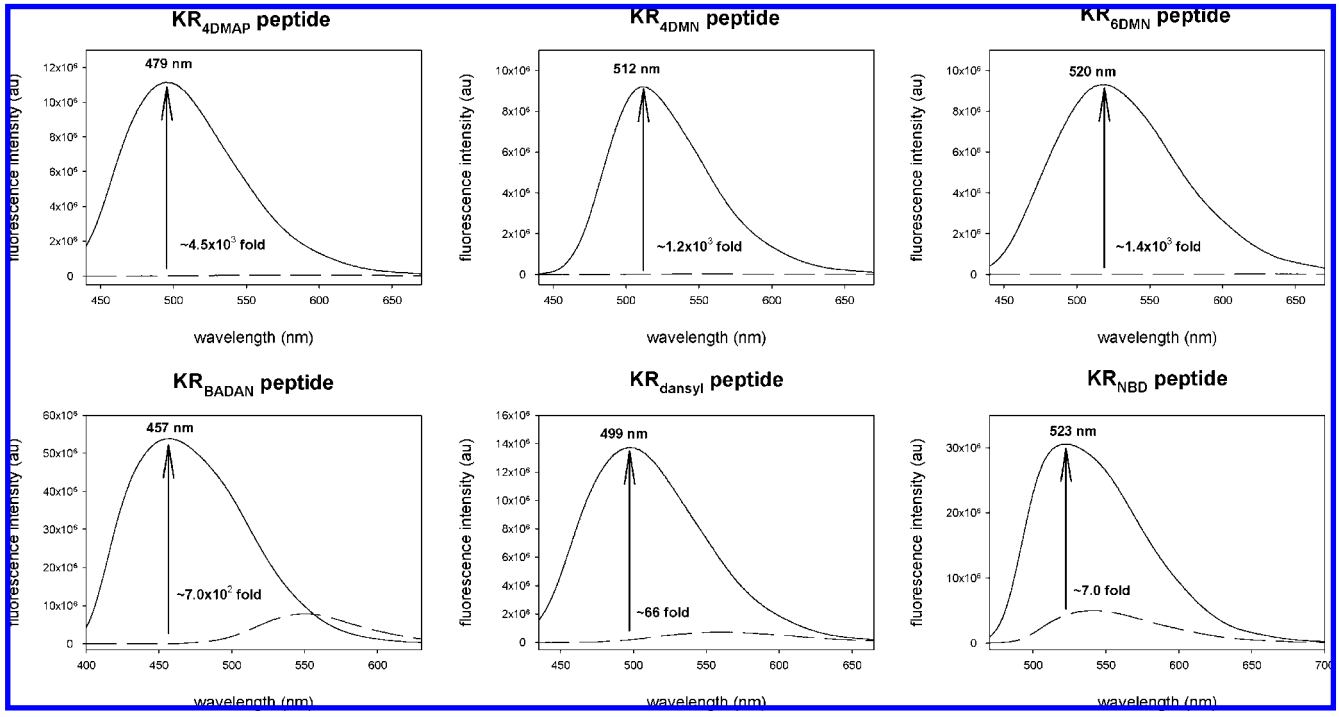


***Figure 4.*** Fluorescence spectra of the KR peptides (5 $\mu$M) measured in TBS buffer at pH 7.4 (− −) and 1,4-dioxane with 5 mM 18-crown-6 (—). Each spectrum is the average of three independent measurements corrected for background. The fold-increase in fluorescence is reported at the wavelength of maximum emission in the 1,4-dioxane solution. All measurements were made at 25 °C.

***Table 2.*** Mutant M13 Peptide Series Containing the Solvatochromic Fluorophores

| | | residue no.[a] | | | | | | | | | | | | | | | | | | |
|---|---|---|---|---|---|---|---|---|---|---|---|---|---|---|---|---|---|---|---|---|
| M13 mutant | N-term | 2 | 3 | 4[c] | 5 | 6 | 7 | 8[b] | 9 | 10 | 11 | 12 | 13 | 14 | 15 | 16 | 17[c] | 18 | 19 | C-term |
| $M13_{4DMAP}$ | $H_2N$- | R | R | **W** | K | K | N | Dap(4DMAP) | I | A | V | S | A | A | N | R | **F** | K | K | -$CONH_2$ |
| $M13_{4DMN}$ | $H_2N$- | R | R | **W** | K | K | N | Dap(4DMN) | I | A | V | S | A | A | N | R | **F** | K | K | -$CONH_2$ |
| $M13_{6DMN}$ | $H_2N$- | R | R | **W** | K | K | N | Dap(6DMN) | I | A | V | S | A | A | N | R | **F** | K | K | -$CONH_2$ |
| $M13_{Dansyl}$ | $H_2N$- | R | R | **W** | K | K | N | Dap(dansyl) | I | A | V | S | A | A | N | R | **F** | K | K | -$CONH_2$ |
| $M13_{NBD}$ | $H_2N$- | R | R | **W** | K | K | N | Dap(NBD) | I | A | V | S | A | A | N | R | **F** | K | K | -$CONH_2$ |
| $M13_{BADAN}$ | $H_2N$- | R | R | **W** | K | K | N | Cys(BADAN) | I | A | V | S | A | A | N | R | **F** | K | K | -$CONH_2$ |

[a] The residue numbering refers to the original M13 fragment reported by Blumenthal et al.[41] [b] The fluorophore, indicated in parentheses, is appended to the 3-amino group of Dap or, in the case of the $M13_{BADAN}$ mutant, the side chain of the cysteine residue. The wild-type M13 peptide contains a phenylalanine residue at this position. [c] Trp 4 and Phe 17 (bold face) are the key residues that bind in the hydrophobic pockets of the C- and N-terminal domain, respectively, forming important contacts that may establish the orientation of the α-helical peptide in the complex.[47]

that CaM is tolerant of most hydrophobic residues at this position.[47] The mutant M13 peptides of Table 2 represent abridged versions of the original 27-residue M13 peptide reported by Blumenthal et al.[41] The peptides of this study consist only of the span of residues required for binding. The CaM construct used in this investigation contained a C-terminal hexahistidine tag used for purification and as an epitope for Western Blot analysis. The fluorescence spectra for the mutant M13 peptides were recorded in the presence of saturating CaM, $CaCl_2$, and CaM with $CaCl_2$ (see Supporting Information for details). These results were then compared to the spectra of the peptides alone (Figure 6).

Unlike the previous study that examined the fluorescent properties of the fluorophores in dioxane versus water, the measured spectra in this experiment reflect a complex array of variables extending well beyond solvent polarity. Here, the fluorophores are sequestered within a highly restricted microenvironment upon binding of the M13 peptide mutants to calcium-activated CaM. Such microenvironments lack the homogeneity of a fluid medium of uniform dielectric constant. The packing of each fluorophore within the binding interface is strongly influenced by its size, shape, and hydrophobicity. A deeply buried solvatochromic fluorophore, stripped of a surrounding solvent sphere, will no longer experience the effects of solvent relaxation, which reduces the energy gap between the ground and excited electronic states.[9] The rigidity of the microenvironment can also impact the observed fluorescence quantum yields by restricting certain vibrational modes within the excited-state fluorophore that may lead to the ground state through nonradiative decay processes.[9] Bearing in mind that each fluorophore can respond differently to a particular microenvironment and that the nature of such microenvironments can vary widely depending on the protein interaction of interest, the results of this type of comparative study are relative, and some caution should be exercised when making generalizations. Nevertheless, basic trends do emerge providing guidelines for gauging the efficacy of these tools in future applications.

With the exception of the $M13_{4DMN}$ peptide, all members of this series showed a significantly smaller hypsochromic shift in their emission spectra between the bound and unbound states (Table 3) compared to that observed in water versus dioxane (Table 1) with the corresponding KR peptides. This observation

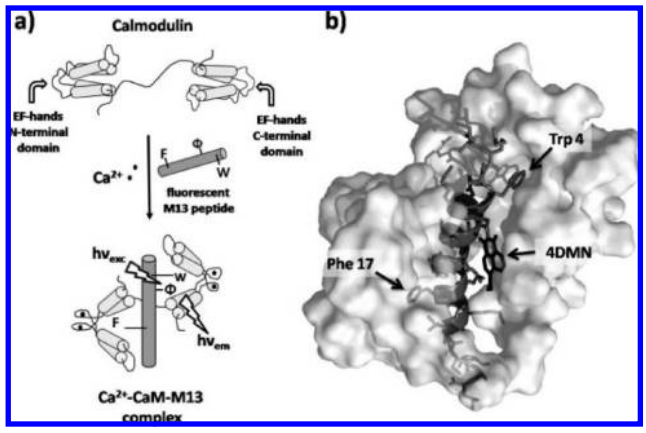


***Figure 5.*** (a) $Ca^{2+}$ activation and binding of CaM (white) to an M13 peptide mutant (gray) that contains a residue with an environment sensitive fluorophore as the side chain (Φ). Upon complex formation, the fluorophore exhibits a measurable change in fluorescence. The Trp 4 and Phe 17 residues are indicated in this panel using the one-letter code notation for amino acids. (b) NMR structure of the $Ca^{2+}$-CaM-M13 peptide complex deposited by Ikura et al. in the Brookhaven Protein Data Bank (2BBM).[42] The structure indicates the solvent-exposed surface of CaM (white) surrounding the M13 peptide (gray). Superimposed over the side chain of residue Phe 8 is 4-DMN (black) as it might be oriented in the $M13_{4DMN}$ peptide mutant.[48]

is fairly typical of environment-sensitive fluorophores, as changes in the local solvent environment are often more subtle in studies of this type. Despite this fact, the dimethylaminophthalimide series still exhibited the greatest overall changes in fluorescence intensity. Furthermore, the $M13_{4DMN}$ peptide produced the most dramatic results, yielding a greater than 900-fold increase in fluorescence in the presence of saturating CaM and $Ca^{2+}$ compared to that of the peptide alone. The magnitude of this change, which was approximately 5−8 times greater than that of 4-DMAP and 6-DMN, may be due to better packing of the fluorophore within the peptide−protein complex.

All of the M13 peptide mutants exhibited small increases in fluorescence intensities in the presence of CaM alone, with the largest change being observed for the $M13_{4DMN}$ peptide (∼9-fold). Initially, this was thought to be the result of some contaminating calcium that was activating a fraction of the total calmodulin toward binding of the fluorescent peptides. However, control experiments that were performed using chelating agents like EDTA to sequester free calcium showed this was not the cause of the observed increases. Rather, it was concluded that the increases in fluorescent signal were due to the weak association constant that exists for the CaM−M13 complex in the absence of calcium. It has previously been reported that the $K_d$ of the CaM−M13 complex is approximately two-million-fold higher than that of the $Ca^{2+}$-CaM−M13 complex.[49] Based on our determination of the $K_d$ of the $Ca^{2+}$-CaM−$M13_{4DMN}$ complex shown in Figure 7, we estimated that the calcium-independent $K_d$ is on the order of 150−200 $\mu$M. This would imply that roughly 7% of the mutant M13 peptide is bound by CaM under these experimental concentrations. Consequently, two different ratios are reported in Table 3: the fluorescence increase upon the addition of calcium when CaM was already present ($I_{(○)}/I_{(△)}$) and the overall fluorescence increase observed when comparing the fluorescence of the $Ca^{2+}$-CaM−M13 complex to that of the M13 mutant alone ($I_{(○)}/I_{(●)}$).

The results of Figure 6 exemplify the importance of having low-background fluorescence for the unbound probe. If the measured hypsochromic shift is small, such that the emission spectrum of the $Ca^{2+}$-CaM−M13 complex partially or fully overlaps with that of the lone peptide, then a large quantum yield of fluorescence in water may drastically limit the magnitude of the measured fluorescence increase. Since the dimethylaminophthalimide series exhibits very little fluorescence in aqueous environments, even a modest shift in the emission wavelength will typically be accompanied by a significant

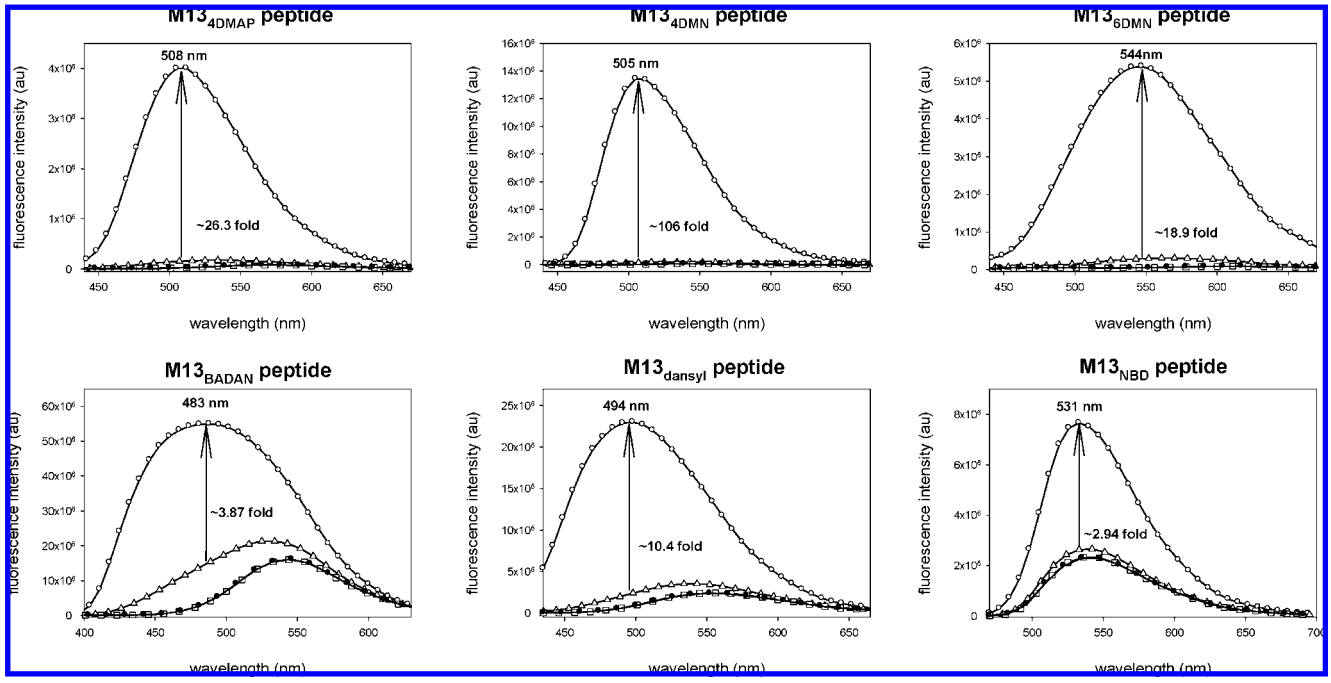


***Figure 6.*** Fluorescence spectra of the M13 mutant peptide series measured in TBS buffer at pH 7.4, 25 °C with EDTA (40 $\mu$M). Four separate conditions were examined for each member of the series shown above: ●, M13 peptide (10 $\mu$M); △, M13 peptide (10 $\mu$M) + CaM (15 $\mu$M); ○, M13 peptide (10 $\mu$M) + CaM (15 $\mu$M) + $Ca^{2+}$ (200 $\mu$M); □, M13 peptide (10 $\mu$M) + $Ca^{2+}$ (200 $\mu$M). Each spectrum represents the average of three independent measurements corrected for background. The fold-increase in fluorescence indicated by the arrows represents the fluorescence ratio between conditions ○ and △ at the wavelength of maximum emission ($\lambda_{em}$) in condition ○.

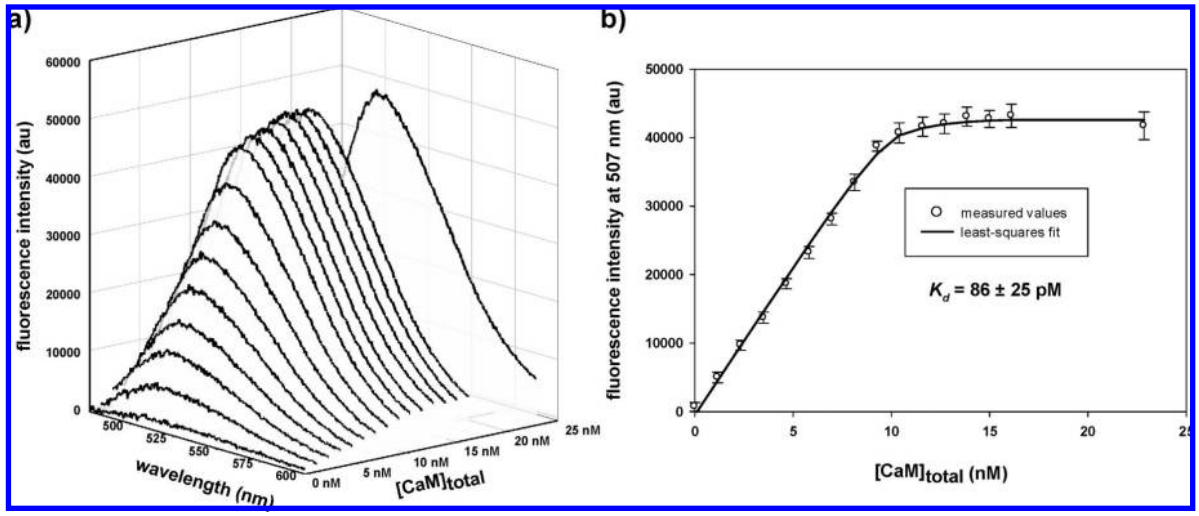


***Figure 7.*** (a) Fluorescence spectra collected from 475 to 600 nm as the $M13_{4DMN}$ peptide (10 nM) was titrated with CaM in the presence of 200 $\mu$M $CaCl_2$. The fluorophore was excited at 408 nm. Each spectrum represents the average of nine measurements after background correction. (b) Titration curve of the $M13_{4DMN}$ peptide measured at 507 nm. The error bars shown for the measured values represent the 95% confidence interval based on the average of nine trials. The solid line indicates the least-squares fit to the measured data. The interval shown for the $K_d$ of the complex was also calculated at the 95% confidence level.

***Table 3.*** Observed Fluorescence Changes for M13 Mutants in the Presence of CaM and $Ca^{2+}$-CaM

| peptide | $\lambda_{exc}$ (nm) | $\lambda_{em}$ (nm), free M13 peptide[a] | $\lambda_{em}$ (nm), $Ca^{2+}$-CaM−M13 complex[b] | $I_{(○)}/I_{(△)}$ at $\lambda_{em}$[c] | $I_{(○)}/I_{(●)}$ at $\lambda_{em}$[c] |
|---|---|---|---|---|---|
| $M13_{4DMAP}$ | 390 | 567 | 508 | 26.3 ± 7.4 | 183 ± 3 |
| $M13_{4DMN}$ | 408 | 550 | 505 | 106 ± 7 | 963 ± 100 |
| $M13_{6DMN}$ | 378 | 608 | 544 | 18.9 ± 1.2 | 119 ± 4 |
| $M13_{BADAN}$ | 365 | 542 | 483 | 3.87 ± 0.05 | 17.9 ± 0.7 |
| $M13_{dansyl}$ | 345 | 553 | 494 | 10.4 ± 0.1 | 33.3 ± 2.3 |
| $M13_{NBD}$ | 455 | 541 | 531 | 2.94 ± 0.14 | 3.41 ± 0.20 |

[a] Measurements made in TBS buffer (pH 7.4, 25 °C) with the M13 peptide concentration at 10 $\mu$M. [b] Measurements made in TBS buffer (pH 7.4, 25 °C) with M13 peptide (10 $\mu$M), CaM (15 $\mu$M), and $CaCl_2$ (200 $\mu$M). [c] The measured fluorescence intensity ratios are indicated by the subscripted symbols: ●, M13 peptide alone; △, M13 peptide + CaM; and ○, M13 peptide + CaM + $Ca^{2+}$. The listed errors represent the 90% confidence interval from an average of three trials.

change in fluorescence intensity. Hence, these probes closely mimic switch-like or "on−off" emission properties making them excellent tools for cell microscopy by eliminating the need for extensive washing to reduce background signal due to unbound probe.[13] Furthermore, these probes may readily be adapted for ratiometric measurements by introducing a secondary nonsolvatochromic fluorophore of a different emission wavelength to afford more quantitative information within the highly compartmentalized environment of living cells.

**Titration of the $M13_{4DMN}$ Peptide with Calcium-Activated CaM.** One caveat of incorporating unnatural structural elements into proteins is the potential to disrupt a native binding interaction. A titration of the $M13_{4DMN}$ peptide with $Ca^{2+}$-CaM was performed to demonstrate that that the presence of the unnatural amino acid, **3**, has a negligible impact on the affinity of the complex (Figure 7). The $K_d$ for the wild-type M13 peptide has previously been reported by several groups using various techniques that place the value within the low nanomolar to high picomolar range.[41,50,51] In this study, the averaged $K_d$ for the $Ca^{2+}$-CaM−$M13_{4DMN}$ complex was determined to be 86 ± 25 pM, indicating an extremely tight interaction (see Supporting Information for details). Therefore, it was concluded that the presence of 4-DMNA at position 8 in the M13 peptide sequence does not significantly impact the protein−peptide interaction.

## Conclusions

While there are a number of known solvatochromic fluorophores that have been developed into amino acids,[10,52−56] it is rare for a single species to meet all of the criteria for obtaining optimal results in protein studies. Tradeoffs often exist between variables such as good extinction coefficients, suitable wavelengths of excitation and emission, thermal and photochemical stability, size, and many others. The 4-DMNA amino acid is distinctive in that this species yields very few compromises by combining many of the key elements required of a good fluorescent tool. It can be excited in the visible spectrum (400−450 nm), thus minimizing the damaging effects of high-energy UV light; the Fmoc building block, **4**, can be prepared in few synthetic steps and offers facile incorporation into peptides; the fluorescent side chain is significantly more stable than those of 4-DAPA and 6-DMNA; and it possesses the same switch-like fluorescent properties that are characteristic of the dimethylaminophthalimide series. Like 4-DAPA and 6-DMNA, the comparative size of 4-DMNA to the natural aromatic amino acids allows it to be incorporated into peptides or proteins without significantly altering the native surface topology. This is critical in developing new fluorescent probes like the

(49) Olwin, B. B.; Edelman, A. M.; Krebs, E. G.; Storm, D. R. *J. Biol. Chem.* **1984**, *259*, 10949–10955.
(50) Gao, Z. H.; Krebs, J.; VanBerkum, M. F.; Tang, W. J.; Maune, J. F.; Means, A. R.; Stull, J. T.; Beckingham, K. *J. Biol. Chem.* **1993**, *268*, 20096–20104.
(51) Findlay, W. A.; Martin, S. R.; Beckingham, K.; Bayley, P. M. *Biochemistry* **1995**, *34*, 2087–2094.
(52) Summerer, D.; Chen, S.; Wu, N.; Deiters, A.; Chin, J. W.; Schultz, P. G. *Proc. Natl. Acad. Sci. U.S.A.* **2006**, *103*, 9785–9789.
(53) Wang, J.; Xie, J.; Schultz, P. G. *J. Am. Chem. Soc.* **2006**, *128*, 8738–8739.
(54) Cohen, B. E.; McAnaney, T. B.; Park, E. S.; Jan, Y. N.; Boxer, S. G.; Jan, L. Y. *Science* **2002**, *296*, 1700–1703.
(55) Turcatti, G.; Nemeth, K.; Edgerton, M. D.; Meseth, U.; Talabot, F.; Peitsch, M.; Knowles, J.; Vogel, H.; Chollet, A. *J. Biol. Chem.* **1996**, *271*, 19991–19998.
(56) Dufau, I.; Mazarguil, H. *Tetrahedron Lett.* **2000**, *41*, 6063–6066.

$M13_{4DMN}$ peptide, which we have shown to have a binding affinity for $Ca^{2+}$-CaM similar to that reported for the wild-type system. The combination of these properties into this single amino acid opens the window to many potential future applications as we aim to incorporate this tool into full-length proteins for *in cellulo* studies.

**Acknowledgment.** This research was supported by NSF CHE-0414243 (BI), the NIH Cell Migration Consortium (GM064346), and the Biotechnology Training Program (T32-GM08334). Special thanks to Dr. M. A. Sainlos (MIT) for his helpful advice and insight. The Department of Chemistry Instrumentation Facility (NSF CHE-9808061, DBI-9729592, and CHE-0234877) and the Biophysical Instrumentation Facility for the Study of Complex Macromolecular Systems (NSF-0070319) are also gratefully acknowledged.

**Supporting Information Available:** Synthesis and characterization of 4-*N,N*-dimethylamino-1,8-naphthalimide derivatives including **4** and **6**; details regarding the preparation and characterization of the KR peptide series and M13 mutant peptide series; cloning and expression of the CaM-His6 construct; protocols for the fluorescence experiments conducted on the KR peptides and M13 mutant peptides; measurement of the kinetics of 4-DMAP and 6-DMN hydrolysis; procedure for examining the reactivity of the dimethylaminophthalimides to 4-methylpiperidine; determination of the extinction coefficient of 4-DMN at 440 nm in TBS buffer (pH 7.4). This material is available free of charge via the Internet at http://pubs.acs.org.

JA804754Y